ARMY RESEARCH LABORATORY

Numerical Study of Head/Helmet Interaction Due to Blast Loading

by Timothy G Zhang, Sikhanda S Satapathy, Amy M Dagro, and Philip J McKee

ARL-RP-0509 **October 2014**

A reprint from the *Proceedings of ASME 2013 International Mechanical Engineering Congress & Exposition IMECE2013*, San Diego, CA, 2013 Nov 15–21.

NOTICES

Disclaimers

Army Research Laboratory
Aberdeen Proving Ground, MD 21005-5069

ARL-RP-0509 **October 2014**

Numerical Study of Head/Helmet Interaction Due to Blast Loading

Timothy G Zhang
Bowhead Science and Technology

Sikhanda S Satapathy and Amy M Dagro
Weapons and Materials Research Directorate, ARL

Philip J McKee
Dynamic Science, Inc.

A reprint from the *Proceedings of ASME 2013 International Mechanical Engineering Congress & Exposition IMECE2013*, San Diego, CA, 2013 Nov 15–21.

REPORT DOCUMENTATION PAGE			*Form Approved* *OMB No. 0704-0188*

1. REPORT DATE *(DD-MM-YYYY)*	October 2014
2. REPORT TYPE	Reprint
3. DATES COVERED (From - To)	January 2013–April 2013
4. TITLE AND SUBTITLE	Numerical Study of Head/Helmet Interaction Due to Blast Loading
5a. CONTRACT NUMBER	
5b. GRANT NUMBER	
5c. PROGRAM ELEMENT NUMBER	
6. AUTHOR(S)	Timothy G Zhang, Sikhanda S Satapathy, Amy M Dagro, and Philip J McKee
5d. PROJECT NUMBER	
5e. TASK NUMBER	
5f. WORK UNIT NUMBER	
7. PERFORMING ORGANIZATION NAME(S) AND ADDRESS(ES)	US Army Research Laboratory ATTN: RDRL-WMP-B Aberdeen Proving Ground, MD 21005-5069
8. PERFORMING ORGANIZATION REPORT NUMBER	ARL-RP-0509
9. SPONSORING/MONITORING AGENCY NAME(S) AND ADDRESS(ES)	
10. SPONSOR/MONITOR'S ACRONYM(S)	
11. SPONSOR/MONITOR'S REPORT NUMBER(S)	
12. DISTRIBUTION/AVAILABILITY STATEMENT	Approved for public release; distribution is unlimited.
13. SUPPLEMENTARY NOTES	A reprint from the *Proceedings of ASME 2013 International Mechanical Engineering Congress & Exposition IMECE2103*, San Diego, CA, 2013 Nov 15–21.

14. ABSTRACT

Recent wars have heightened the need to better protect dismounted soldiers against emerging blast and ballistic threats. Traumatic Brain Injury (TBI) due to blast and ballistic loading has been a subject of many recent studies. In this report, we report a numerical study to understand the effects of load transmitted through a combat helmet and pad system to the head and eventually to the brain during a blast event. The ALE module in LS-DYNA was used to model the interactions between fluid (air) and the structure (helmet/head assembly). The geometry model for the head was generated from the MRI scan of a human head. For computational simplicity, four major components of the head are modeled: skin, bone, cerebrospinal fluid (CSF) and brain. A spherical shape blast wave was generated by using a spherical shell air zone surrounding the helmet/head structure. A numerical evaluation of boundary conditions and numerical algorithm to capture the wave transmission was carried out first in a simpler geometry. The ConWep function was used to apply blast pressure to the 3D model. The blast pressure amplitude was found to reduce as it propagated through the foam pads, indicating the latter's utility in mitigating blast effects. It is also shown that the blast loads are only partially transmitted to the head. In the calculation where foam pads were not used, the pressure in the skin was found to be higher due to the underwash effect in the gap between the helmet and skin, which amplified the blast pressure.

15. SUBJECT TERMS

blast load, head/helmet, head model, foam pads, fluid structure interaction

16. SECURITY CLASSIFICATION OF:			17. LIMITATION OF ABSTRACT	18. NUMBER OF PAGES	19a. NAME OF RESPONSIBLE PERSON
a. REPORT	b. ABSTRACT	c. THIS PAGE			Timothy G Zhang
Unclassified	Unclassified	Unclassified	UU	16	19b. TELEPHONE NUMBER (*Include area code*) 410-306-2984

Standard Form 298 (Rev. 8/98)
Prescribed by ANSI Std. Z39.18

Proceedings of ASME 2013 International Mechanical Engineering Congress & Exposition
IMECE2013
Nov 15-21, 2013, San Diego, California, USA

IMECE2013-63015

NUMERICAL STUDY OF HEAD/ HELMET INTERACTION DUE TO BLAST LOADING

Timothy G Zhang
Bowhead Science and Technology
Belcamp, MD, USA

Sikhanda S Satapathy
US Army Research Laboratory
Aberdeen Proving Ground, MD, USA

Amy M Dagro
US Army Research Laboratory
Aberdeen Proving Ground, MD, USA

Philip J McKee
Dynamic Science, Inc.
Aberdeen, MD, USA

ABSTRACT

Recent wars have heightened the need to better protect dismounted soldiers against emerging blast and ballistic threats. Traumatic Brain Injury (TBI) due to blast and ballistic loading has been a subject of many recent studies. In this paper, we report a numerical study to understand the effects of load transmitted through a combat helmet and pad system to the head and eventually to the brain during a blast event. The ALE module in LS-DYNA was used to model the interactions between fluid (air) and the structure (helmet/head assembly). The geometry model for the head was generated from the MRI scan of a human head. For computational simplicity, four major components of the head are modeled: skin, bone, cerebrospinal fluid (CSF) and brain. A spherical shape blast wave was generated by using a spherical shell air zone surrounding the helmet/head structure. A numerical evaluation of boundary conditions and numerical algorithm to capture the wave transmission was carried out first in a simpler geometry. The ConWep function was used to apply blast pressure to the 3D model. The blast pressure amplitude was found to reduce as it propagated through the foam pads, indicating the latter's utility in mitigating blast effects. It is also shown that the blast loads are only partially transmitted to the head. In the calculation where foam pads were not used, the pressure in the skin was found to be higher due to the underwash effect in the gap between the helmet and skin, which amplified the blast pressure.

1. INTRODUCTION

The incidence of Traumatic Brain Injury (TBI) due to blast loading has emerged as a leading concern for military personnel in recent years. The performance of helmets is better characterized against ballistic loads as compared to blast loads [1][2]. In both cases, the load transmitted to the brain through the helmet/pad system and its effect on structural and functional changes in the brain are of interest, and have been a subject of recent investigations [3].

Experimental investigations on human cadavers as well as animal models [4] have produced useful information on stress wave propagation and consequent injury to the brain tissues. However, since experiments can obtain measurements only at limited locations and duration, numerical analysis provides a complementary avenue to assess structural response of the brain at greater spatial and temporal resolution. The numerical tools require careful evaluation of the constitutive response of constituent tissues, and appropriate experimental results for calibration and validation of model parameters. Constitutive model development for brain tissue and relevant experimental work, even though incomplete currently, has been the subject of intense research. In this study, we use available data from the literature to evaluate interaction between head/ helmet system and the resulting stress wave transmission under a few representative scenarios.

Interactions between air blast and helmet/head require use of Arbitrary Lagrangian Eulerian (ALE) methods to model the

fluid/ structure interaction [5]. The loading on the helmet from the air-blast can also be modeled by using explicit loading functions, such as ConWep, which is computationally more efficient than using ALE for full fluid/ structure interaction. However, the disadvantage of ConWep blast function is its inability to account for confinement or shadowing. Therefore, this method is unable to capture the underwash effect in the gap between the helmet and head. An intermediate option is to use ConWep boundary conditions to the boundary of the air surrounding the structure, obviating the need to model the larger air-volume that includes the explosive. The finite element code, LS-DYNA [6], offers such an option, and was used in our computations.

The head geometry for our study was obtained from a MRI scan of a human head. The ECH helmet and foam pads geometry are representative of currently used helmet systems, and were meshed with hex elements. The air surrounding the helmet/head assembly was modeled to capture the interactions between the blast and structures, including the underwash effects inside the helmet. A blast loading is applied to the air boundary. The model was exercised to simulate the blast loads transfer to human head with the protection of a helmet. Material failure is not modeled in the present study.

The case when foam pads are not used between the helmet and skin was also studied. In the study reported in [7], a gap is put between the helmet and skin, which is representative of a web-suspension system for the helmet. Presence of the gap leads to a longer time for the helmet to possibly hit the skin under blast loading. This time delay leads to an undesirable consequence for the model size requirement for the air. A larger air zone needs to be used to avoid wave reflections from the boundary that would contaminate the solution in the head/ helmet region. A larger air zone size also leads to a higher computational burden. In addition, the helmet motion with web-suspension would be different from the case with a pad or a gap. Therefore, to compare the effect of foam pad between the helmet and the skin, a different approach is taken in our study, where the initial gap is removed between the helmet and the skin. Such comparative study would be helpful to understand the magnitude of the impact force by the direct helmet hit.

A simpler 2-D problem is first studied before simulating the more complex 3D model to explore available numerical algorithms and to understand the wave reflection and transmission at different material interfaces. Identical material parameters are used in both models. The suitability of ALE and Lagrangian methods for the CSF is investigated using the 2D model.

2. NUMERICAL MODEL

The main goal of this study is to investigate the effect of helmet/pad on the load transfer and subsequent pressure propagations inside the head. This is a very challenging problem due to the complex geometry, sensitivity of the material models, and limitations inherent in the numerical methods. Only one half of the geometry is modeled to take advantage of sagittal symmetry. The blast loading is applied from the frontal direction of the head.

2.1. Geometry

The Enhanced Combat Helmet (ECH) (Figure 1) geometry was obtained from the PEO-Soldier's office and was simplified for modeling expediency. The helmet rim, coating layer, holes/bolts and retention system are not included in our model. We focused on the response of helmet/head within 4-5 ms after the blast wave arrival. To study the response beyond 5 ms of the head and helmet, the retention system and boundary condition of the head will need to be considered in the future.

Figure 1: ECH helmet with strap [8]

Seven pads (foam covered by fabric shell) in three different shapes are attached to helmet shell through hook disks. When soldiers wear the helmet, the pads deform due to the helmet weight, and conform to the head shape. Therefore there is initial state of stress and deformation in the foams. In our model, the hook disks are ignored, and no gap is assumed between the pads and helmet shell or between the pads and the head, as shown in Figure 2. No initial deformation and stress is applied to the foam pads.

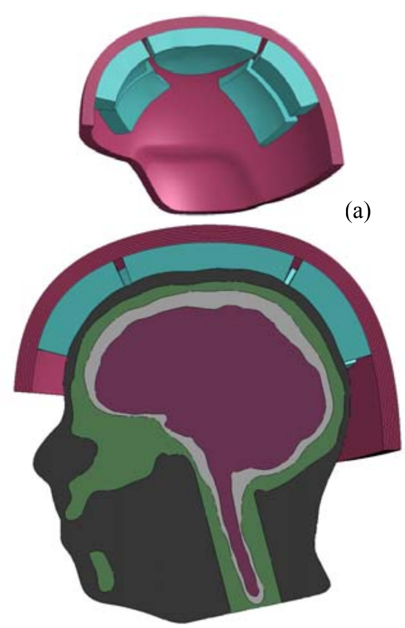

Figure 2: Geometry in our model (a) helmet/pad, (b) helmet/head assembly (half model is used)

The head geometry is generated from the MRI scan of a human head. For computational simplicity, four major components of the head are modeled: skin, bone, cerebrospinal fluid (CSF) and brain (they are shown in black, green, white and purple, respectively, in Figure 2 (b)). Complex topological features of the brain are simplified for computational convenience. The nose and eyes are filled with skin material; the white matter, grey matter, cerebellum and brain stem are modeled as a single material of brain. Therefore the interactions between the sub-components such as white matter and grey matter, sulci/ gyri and CSF, are ignored in our calculation.

The skull is connected to the body through seven cervical vertebrae and six cervical disks. Only the head/neck is modeled with appropriate boundary conditions. Within short time period (~5 ms), the head movement is small and the complex cervical geometries are simplified into a cylinder, as shown in Figure 2. The skull, lower jaw and the cervical vertebrae are modeled as a single bone material, which is shown in green in the Figure 2.

2.2. Material Model

The foam pads for the ECH are comprised of two layers of foam: a hard and a soft layer, with a fabric covering. The hard foam is known as the impact liner, while the soft foam is the comfort liner adjacent to the head. The two foam layers are modeled as one material with average properties using the MAT_CRUSHABLE_FOAM in LS-DYNA to model the foam behavior. The stress-strain curves from [2] are used for the foam pads properties.

The helmet shell is made of Ultra-High-Molecular-weight polyethylene fibers. It is made of 0/90º plies of unidirectional laminate sheets. The MAT_162 material model in LS-DYNA is used to account for the effects of strain rate and strain softening after damage initiation. Contacts are defined between adjacent layers to model potential delaminations. To be more efficient, 0/90 cross-ply is modeled into one orthotropic layer rather than two layers (a 0 layer and a 90 layer).

The skin is modeled as an elastic material. Its mechanical properties are reported to vary a lot in the literature. For example, the Young's modulus varies from 0.0045 to 150 MPa **[9]** in in-vitro tests. The density, Young's modulus and Poisson's ratio used in our work are [10]

ρ = 1130 Kg/m^3, E = 16.7MPa, ν = 0.42, respectively.

Similarly, an elastic model is used for the skull with density of 1710 Kg/m^3, Young's modulus of 5.37 GPa and Poisson's ratio of 0.19 [7].

Brain is modeled as a viscoelastic material [7]. The properties are,

ρ = 1040 Kg/m^3, K = 2.19 GPa,

G_0= 41 KPa, G_∞= 7.8 KPa, β = 700 $/s$

where K, G_0, G_∞ and β are bulk modulus, short-term shear modulus, long-term shear modulus and decay constant, respectively.

Gruneisen equation of state is used to model the volumetric response of CSF. The constants for water are used [11] for CSF, which are,

ρ = 1000 Kg/m^3, C =1484 m/s,

S_1=1.979, γ_0 = 0.11

where C is the bulk sound speed, S_1 is the slope of particle-speed and shock-speed curve, γ_0 is the Gruneisen coefficient.

The cavitation pressure in water is reported in [12], to be around -27 MPa under shock wave. However, the cavitation pressure can vary from -0.1 MPa for distilled water saturated with air to -20 MPa for distilled water degassed at 0.02% saturation under acoustic wave [12]. This suggests that the cavitation pressure might be higher under shock loading conditions. For most experiments, the cavitation pressure for water is reported to be between -1 MPa and 0.1 MPa due to existence of cavitation nuclei [13]. The cavitation pressure level for CSF was found to have a significant effect on the transmitted stress in the CSF and brain.

In this work, -0.1 MPa is chosen as the cavitation pressure [11] [14] for CSF, i.e., the negative pressure in CSF has a limit of - 0.1 MPa. But our model does not account for the cavitation process or the cavity evolution. Cavity collapse can produce additional pressure spikes, which may cause additional damage to brain tissues.

2.3. The Blast Load and Choice of Algorithm for CSF

The blast wave loading of the head/ helmet can be simulated in two ways: (a) the explosive and air covering the explosive and structures are simulated; (b) only a smaller air region surrounding the head is simulated with pressure loading function (ConWep) applied to the air boundary. Of course, modeling only the air around the head/helmet will be more efficient (usually the explosive is several meters away from the head and hence, modeling of the explosive and the air would require a lot of computational resource). Similarly, the CSF can be modeled either as Lagrangian or ALE part. If the deformation in the CSF is small, it can be modeled as a Lagrangian part, either sharing nodes with adjacent parts or interacting with them by defining contacts.

In view of the above, a simplified model is constructed to evaluate various options before the full 3D model is exercised. In the simplified model, as shown in Figure 3, the geometry consists of cylindrical layers of head components; the helmet and foam are not modeled; a plain strain condition is assumed. The intent is to understand how the pressure loading is propagated and reflected at different material interface, and to identify a suitable numerical algorithm for the CSF. There is

no underwash effect for this problem, therefore the simplest way is to apply the blast loading directly to the structures (all parts are modeled as Lagrangian), as shown in Figure 3. Two additional calculations were done, in which the air surrounding the structure was modeled using ALE solver in LS-DYNA. Second-order advection method was chosen for the ALE calculations.

The CSF was modeled as Lagrangian part in one method and as ALE part in the other, as shown in Figure 4. The air zone dimensions are 0.8 m in length and 1 m in height. All of the different parts share nodes at their interfaces.

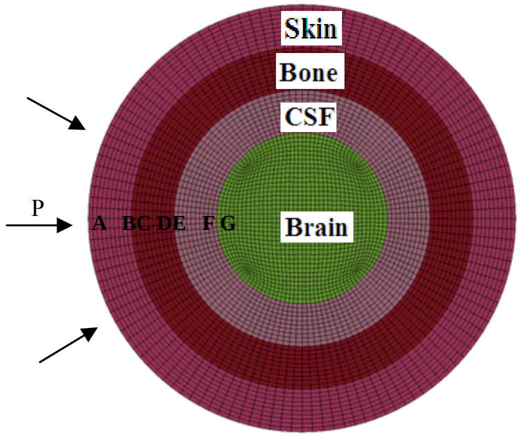

Figure 3: Lagrangian model

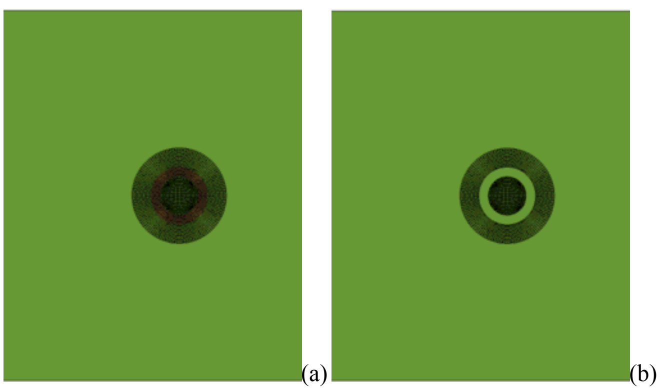

Figure 4: ALE model (a) ALE for air only (b) ALE for CSF and air

The ALE mesh size was 3 mm, the structural mesh size was about 2.5 mm in the radial direction. A charge of 0.1 Kg TNT was placed 3 meters away from the structure. According to the ConWep function, the blast wave at the structure should have 20.7 KPa incident and 44.5 KPa total overpressure[1] (the sum of incident and reflected pressure) with 1.7 ms positive duration.

Pressure time histories at four different locations in the air ahead of the structure are plotted in Figure 5 for models corresponding to Figure 4. Position 1 and 4 are at the left boundary of air and right ahead of the structure. The arrow signs in the figure show the wave propagation directions. Wave 1 is the pressure applied to the air boundary. Wave 1 has a positive duration of 1.68 ms. As the wave propagates towards the structure, the peak pressure decreases slightly. When it arrives at the structure, the pressure is reflected, which has a 42.3 KPa peak. Both the positive duration and reflected overpressure are very close to the analytic solutions. Better agreement can be achieved with a finer mesh. This validates the concept of only modeling the air surrounding the structure to simulate the blast wave.

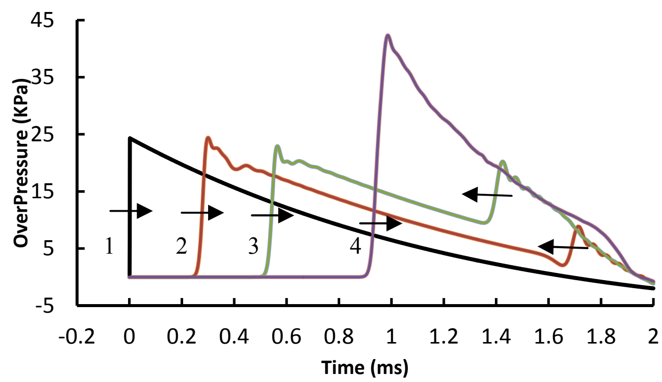

Figure 5: Pressures at different locations in the air ahead of the structure (ALE for CSF and air)

The pressure time histories at seven typical locations (as shown in Figure 3), are plotted in Figure 6 for the three calculations described above. A and B are the locations where the pressure wave enters and leaves the skin, locations C and D, where the pressure wave enters and leaves the bone, locations E and F in CSF material, and location G is where the pressure enters the brain material. When the blast loading is directly applied to the skin surface, it is steep but oscillating. When the air is modeled, the pressure front is less steep (the rise time is longer and the peak is lower.)The pressure increases as it enters bone from skin material (bone has higher acoustic impedance), as seen for curves B and C. As the pressure wave arrives at the interface between the bone and CSF (CSF has lower acoustic impedance), the incident compressive stress reflects as tension due to reduction in acoustic impedance.

The pressures in the skin are similar for all the three methods. However, if the CSF is modeled into ALE meshes, the pressure entering the CSF is much lower and the pressure reflected at the CSF/ bone interface is much higher due to the coupling difference at the CSF/ bone interface. The pressures in the CSF are pretty similar when the CSF is modeled as a

[1] In the literature, the term "reflected pressure" is used sometimes to mean the total pressure obtained after the incident wave reflects from a surface. In this paper, we use "reflected pressure" to indicate the component of pressure that is reflected, and the term "total pressure" is used to indicate the sum of the "incident pressure" and the "reflected pressure," which is what a pressure probe would measure at the interface.

Lagrangian part whether the air surrounding the skin is modeled or not.

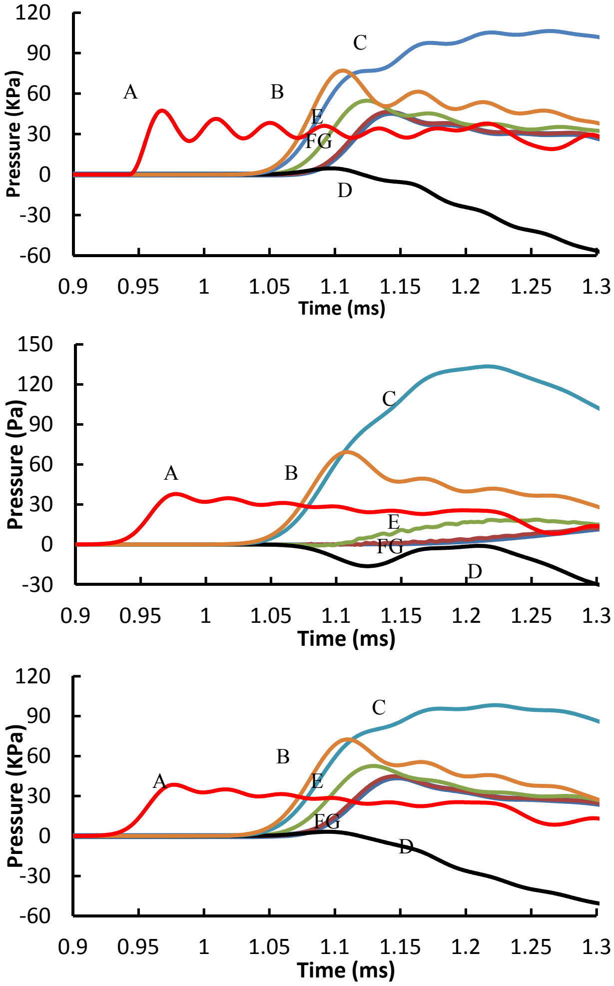

(a)

(b)

(c)

Figure 6: Pressure time histories at different locations for (a) Pure Lagrangian, (b) ALE for CSF and air (c) ALE for air only

As the ALE mesh size in the wave propagation direction is reduced in half, the pressure wave becomes steeper as shown in Figure 7. This is to be expected, since the pressure front is usually distributed across several elements, hence reducing the element size reduces the front width. The finer mesh results are closer to the pure Lagrangian case shown in Figure 6 (a).

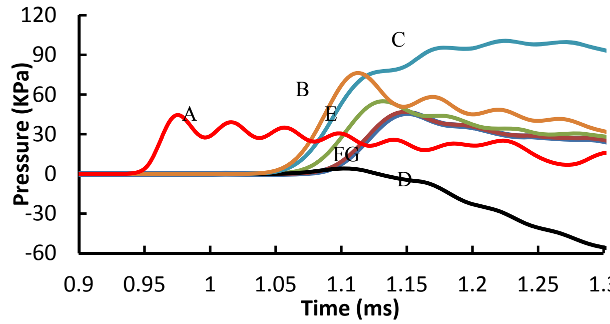

Figure 7: Pressure time histories at different locations for ALE for air only (finer meshes)

Based on the above results, the CSF was modeled as Lagrangian part in the full 3D head/helmet problem described in the following section.

2.4. Model of Helmet/Head Assembly Subjected to Blast Loading

For the full 3D model, TNT explosive of 3.2 Kg was detonated at the head height 3 m away. The peak overpressure is about 26 psi, and the positive phase duration is 2.8 ms. The charge size and distance were chosen not to cause lung damage to human [15]. The blast wave travels into the air zone from the left boundary, i.e., travels along negative y direction, as shown in Figure 8.

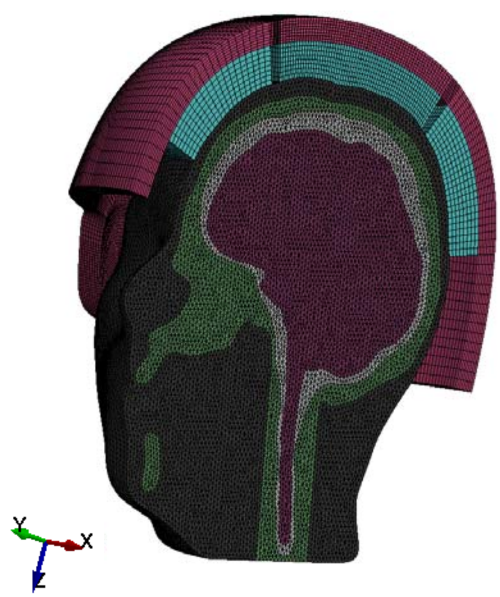

(a)

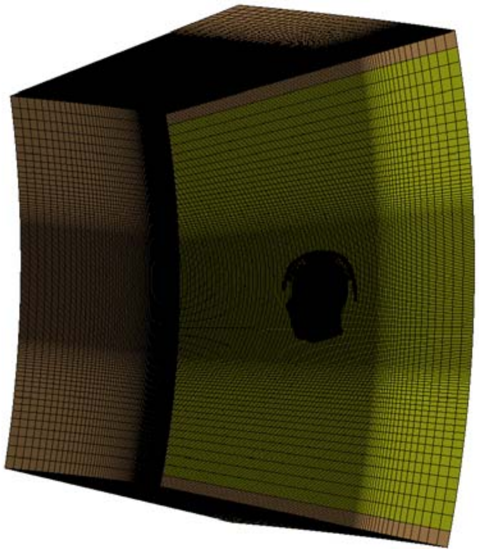

(b)

Figure 8: Meshes for (a) head/helmet, and (b) air (half model is used)

The air surrounding the head/helmet was modeled as ALE part. However, the air zone size has an effect on the accuracy of the loadings to be applied to the structures. **Figure 9** shows the pressure contour in the air of the 2D problem studied in Section 2.3, where a rectangular mesh was used for the air material. At 0.1 ms, the blast wave enters the air and the shock front has a spherical shape. The arrow signs show the wave propagation directions. The shock waves propagate and reflect from the structures. The reflected waves were well captured, as stated above. However, there are two disadvantages of applying ConWep loading function to the boundary of the air with rectangular ALE meshes, namely, the wave shape behind the pressure front is not spherical, and the release waves propagate from the top and bottom air-boundaries. The first is mainly due to unaligned air meshes with the blast wave shape. The latter artifact is also reported in [16]. This effect is related to the boundary conditions. The top and bottom air boundaries have non-reflecting boundary conditions. However, this boundary condition in LS-DYNA only applies to acoustic waves.

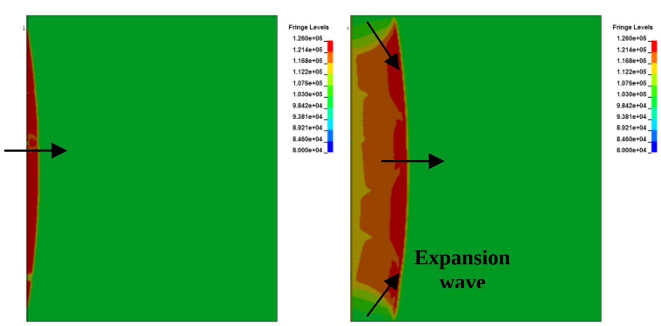

(a) (b)

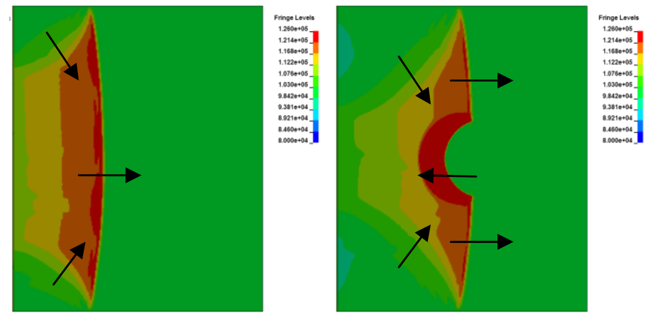

(c) (d)

Figure 9: Pressure contour of the air at time (a) 0.1, (b) 0.5, (c) 0.8 and (d) 1.2 ms

These two issues change the loading applied to the structures. A spherical shell of air zone surrounding the head model, as shown in Figure 8 (b), is used to resolve these issues. The mesh edges are aligned with the blast wave propagation direction. Replacing non-reflecting boundary conditions with ConWep loading to the top and bottom boundaries eliminated the expansion. This will be clear from the results shown in the next Section. If a ConWep loading were to be applied to the top and bottom boundaries of rectangular air zone, the loading would not be realistic since the loading arrival time and magnitude are determined by distance from the explosive (shadow effect is not accounted for).

The air zone size was selected so that the reflected waves from the boundary would not come back to the head during the time period of our interest (5 ms). Since the air far away from the head is not important, coarser mesh was used away from the head. The number of total ALE hexahedral elements was about 2.5 million. The ConWep loading was applied directly to the external air surfaces (brown in Figure 8) except the symmetry plane and the spherical surface on the opposite side of the blast. Only half model is used due to symmetry, and the front side is the sagittal symmetry-plane.

The head (skin/bone/CSF/brain) and helmet (shell/pads) are modeled as Lagrangian parts. The helmet shell and foam pads are discretized into hex elements, while the head components are discretized into tetrahedral elements due to the complex geometry. The pads share nodes with inner helmet shell. A contact is defined between the pads and skin. The skin, bone, CSF and brain share nodes at their interface. The total number of Lagrangian elements is about 1 million.

The Fluid Structure Interaction (FSI) is modeled using the keyword *CONSTRAINED_LAGRANGIAN_IN_SOLID.

Free boundary conditions are applied to the bottom surface of bone, which is used to represent the neck. For a longer response beyond 5ms, appropriate boundary conditions need to be applied.

3. RESULTS

3.1. Case with Foam

The pressure time histories in the air are shown in Figure 10. It can be seen that there are no expansion waves generated from the air boundaries. Since the pressure is applied to the boundary layer (or ambient layer in LS-DYNA) and ambient element must have adjacent air element, corner elements (intersection between two boundary layers) cannot be chosen as ambient elements; there is no pressure applied to the corner and lower pressures are predicted at the corners. However, since the corner elements are far away from the structure, this effect is not a major concern.

With the spherical shell air zone used in the model, the blast wave has a spherical shape. The blast wave arrives at the head/helmet around 0.7 ms and is reflected. The total pressure is the sum of the incident and reflected pressure, which is applied to the structure. The reflected wave propagates toward the air boundary at which it reflects again. Before the waves reflected from the air boundary arrive at the structure, the pressure applied to the skin is accurate. If solution at longer time is desired, a larger air zone needs to be used.

In the gap between the helmet and skin, underwash occurs (see Figure 10(d), around 1 ms). The pressure loading applied to the skin is amplified compared to the cases without gap or helmet. The blast wave travels around the helmet/head and meets again behind the head.

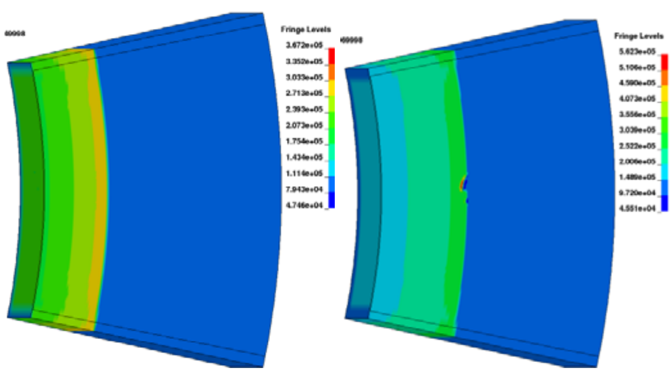

(a) (b)

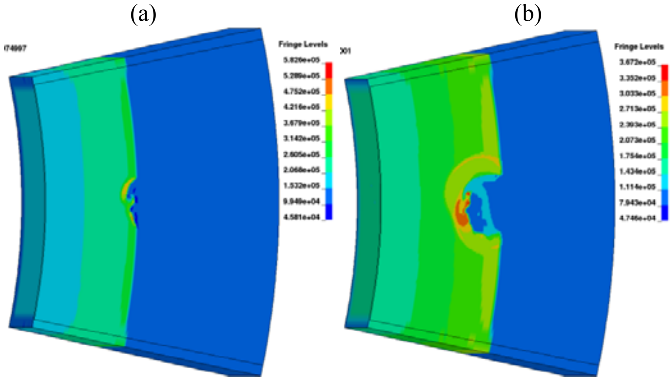

(c) (d)

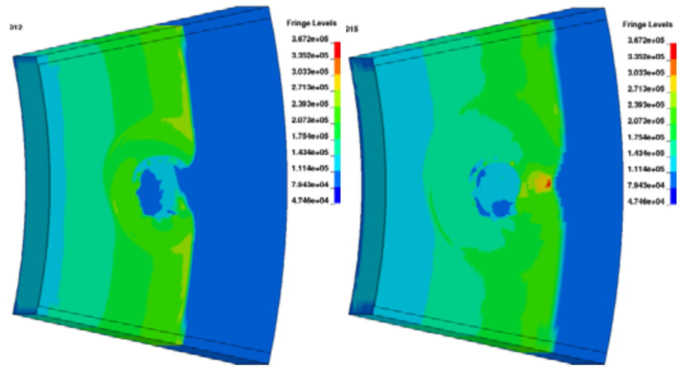

(e) (f)

Figure 10: Pressure time histories in the air at (a) 0.5, (b) 0.7, (c) 0.75, (d) 1.0, (e) 1.2 and (f) 1.5 ms

Figure 11 shows the locations for pressure and y-displacement plots in the remaining, unless specified. Different locations in the air for pressure plot are labeled in Figure 11(a), while some typical locations for y displacement plot in the helmet, foam, bone and brains are given in Figure 11(b).

Figure 12 shows the pressure time histories at different locations in the air. A blast loading of 240 KPa peak overpressure with a 2.5 ms positive duration enters the air at the left boundary of the air-region. When the blast wave arrives at the helmet and nose, it is reflected and the total overpressure is about 320 KPa. The pressure in the gap between helmet, foam and skin are amplified compared to cases without gap.

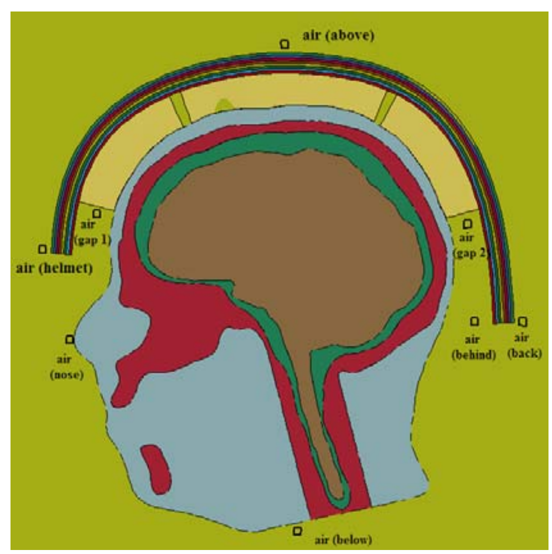

(a)

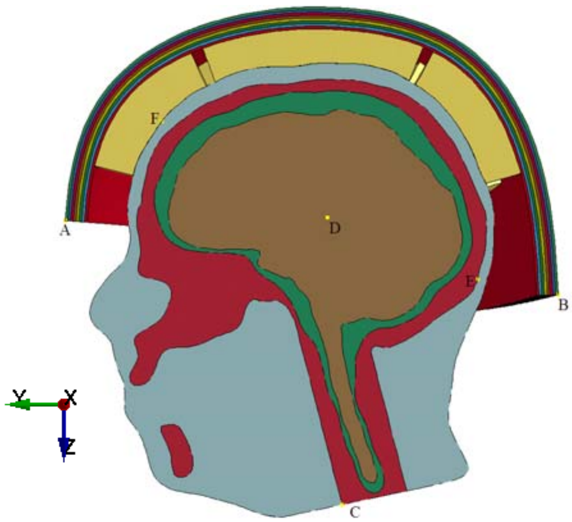

(b)

Figure 11: The schematic of locations for (a) pressure (b) y displacement

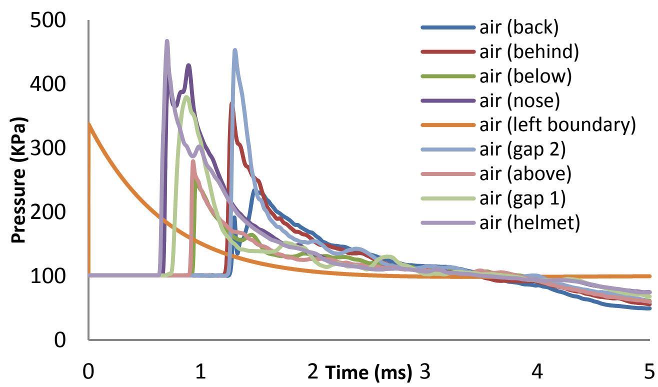

Figure 12: Pressure in the air at different locations

Figure 13 shows the deformation in the helmet/head. At 1 ms, the foam already starts to deform under the blast pressure (which arrives at the foam around 0.75 ms, see Figure 12 curve air (gap 1)). However, the foam first deforms under the compression from the helmet shell under the pressure from the left. This can be seen from the time history of y displacement at location F given in Figure 14. The blast propagates toward negative y direction. The force transmitted through the helmet decreases as the blast loading drops. The maximum negative displacement at location F is about 0.2 mm around 1 ms. When the compression force from the helmet shell drops below the compression force from the air pressure in the gap, the foam starts to deform in the y direction (reverse to the blast direction). The maximum displacement is about 3.8 mm at 1.5 ms. A gap between the foam and skin is formed since the head always has a negative y displacement. Due to the existence of the gap, the blast loading applied to the helmet shell cannot be transmitted to the skin. Therefore, only partial blast loads (prior to gap formed) is transferred to the skin. This can reduce the loading to the skin, but the blast pressure in the gap can also be amplified. The net force will determine whether the helmet with foam can mitigate the blast pressure.

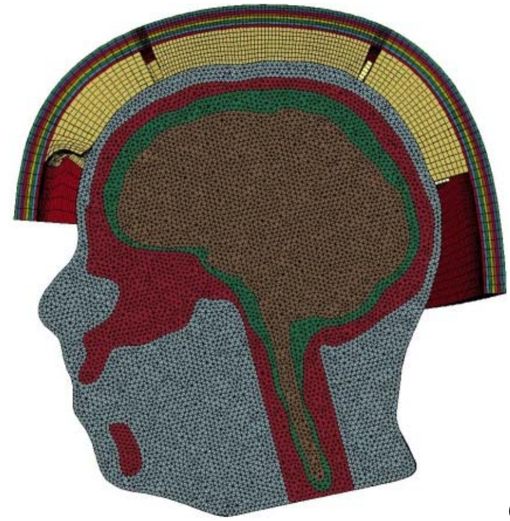

(a)

(b)

Figure 13: Deformations in the helmet/head for (a) 1 ms and (b) 4 ms

The foam shares nodes with the helmet shell in our model. The foam would deform more easily along the interface if the nodes were not shared. In the ECH, the foam is covered by a fabric shell, most of which is attached to the helmet shell through hook disks. If the fabric cover is modeled, the foam can deform parallel to helmet shell and the gap between the foam and skin might not initiate. This will be studied in the future.

It can be seen from Figure 14 that, the helmet shell deflects much more than the head due to the foam between them. The neck also has a larger displacement than the brain.

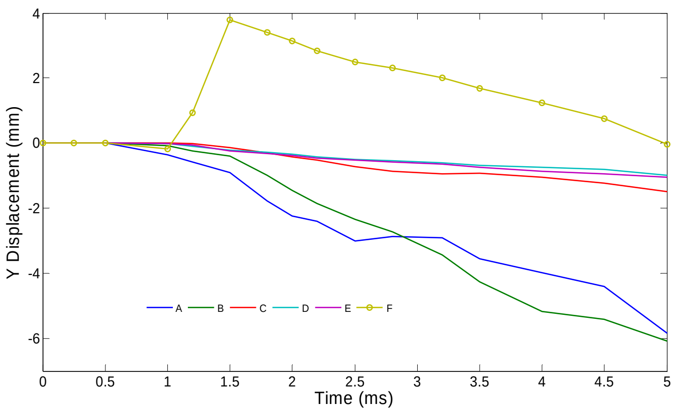

Figure 14: The time histories of y displacements at different locations in the head

Figure 15 shows the pressure time histories in the foam pad ahead of the skin. Path F1-F2 is perpendicular to the helmet shell. It can be seen that the pressure decreases as it propagates in the foam towards the head until the blast pressure arrives from the gap around 0.83 ms. The pressure peak drops from 20 KPa to 10 KPa. This shows that the foam can mitigate the pressure.

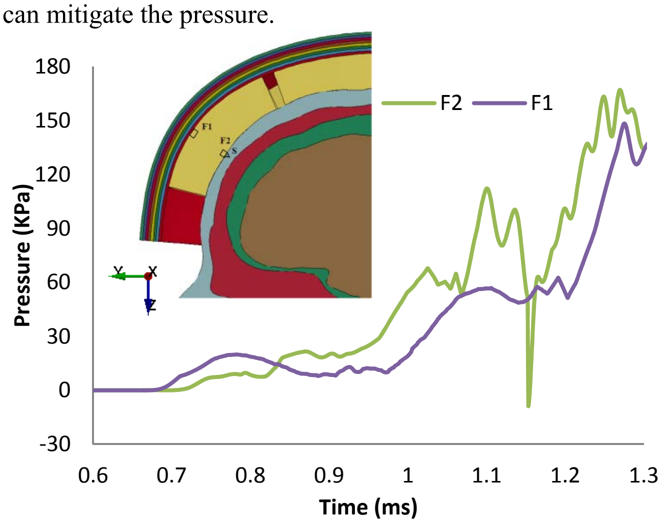

Figure 15: The pressure time histories in the foam

3.2. Case without Foam

We also studied a case when the foam is taken out (the helmet moved vertically down under gravity until it touches the head), as shown in Figure 16.

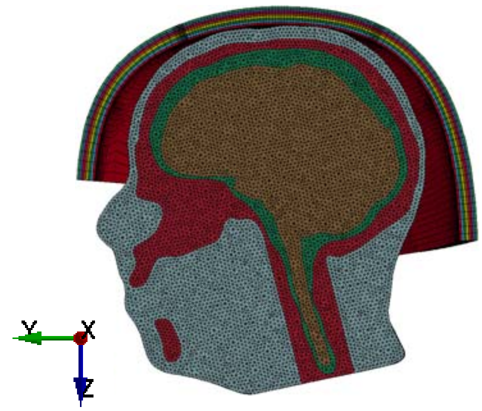

Figure 16: Helmet/head assembly without foam pads

The helmet does not impact the skin within 5 ms in our calculation. The helmet does not deform much and mainly slides on the head. However, the helmet might impact the head due to localized deformations if it is impacted by a bullet.

Figure 17 shows the y displacements at different locations. The helmet can slide more easily from the skin when there is no foam between them. When the foam is put between them, the foam transfers some load to the skin, resulting in higher deflection in the head.

However, the retention system is not modeled in this work. As the helmet starts to slide on the head, the strap will restrain its movement. This will probably make the helmet transfer more loads to the head, and the head will move more together with the helmet. The strap will be included in our future work.

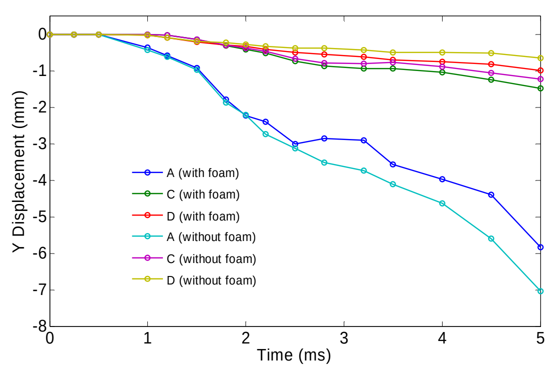

Figure 17: The y displacement at different locations with and without foam pads

Figure 18 compares the pressure in the skin with and without foam pads. The blast pressure is applied to the skin (location S, see Figure 15) directly when there are no foam pads. But the pressure in the skin is transmitted from the foam when foam pads are used, and it is lower compared to the case without foam. This is the case before a gap occurs between the foam and skin. Therefore, the use of foam pads between the helmet and head can mitigate the blast loadings.

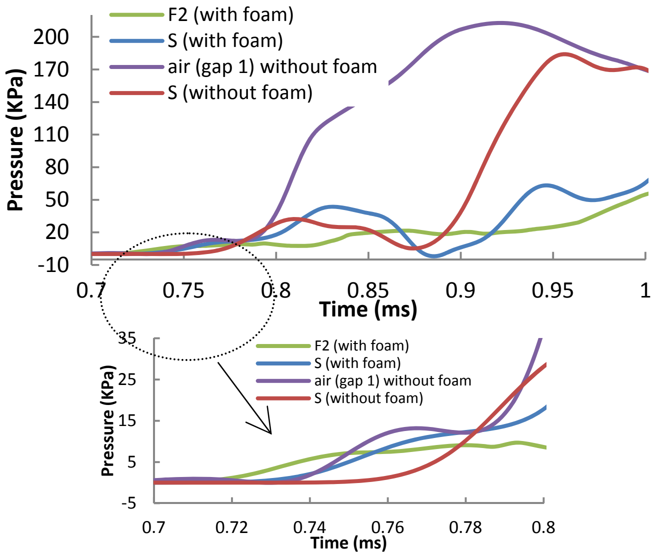

Figure 18: The pressure time histories in the skin

However, the y displacement in the skin (next to location F, see Figure 11(b)) is lower after about 1.2 *ms* without foam, as shown in Figure 19. This is due to higher pressure applied to the back part of the skin, as shown in Figure 20. Dashed lines denote the pressures when no foam pads are used.

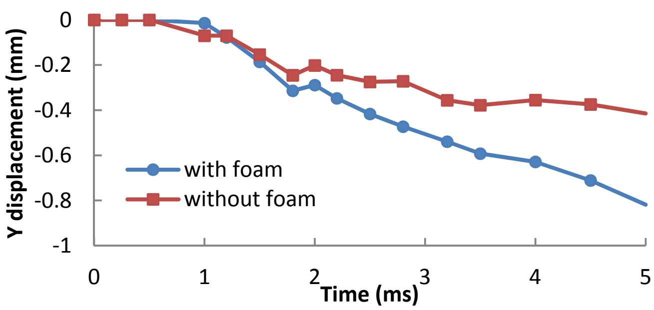

Figure 19: The time histories of y displacement in the skin with and without foam pads

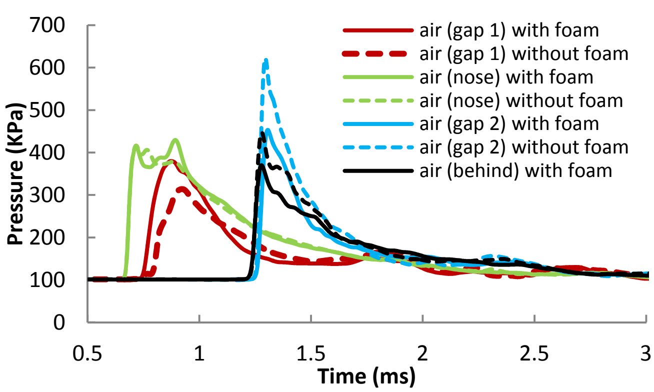

Figure 20: The pressure comparisons in the air with and without foam pads

4. SUMMARY AND OBSERVATIONS

A numerical model to study the blast loading of the head was developed. Certain simplifications were made to the head geometry and the helmet system. A spherical shell shape was used for the air zone surrounding the head, and the ConWep loading function was used to simulate the blast loading at the boundaries. Based on the calculations, the following observations were made.

(1) A Lagrangian description was found to describe the CSF behavior more satisfactorily than an ALE description. In the latter, the load transferred from the bone to the CSF was underestimated.
(2) The use of a spherical shell air zone surrounding the structure eliminated the spurious expansion wave from the air boundary. A spherical blast wave shape was realized. This method enables a more realistic blast loading applied to the structure.
(3) The blast load is partially transmitted to the head through the helmet/pad, i.e., the blast load is transferred to the skin until a gap occurs between skin and the pad.
(4) The foam pads reduce the transmitted pressure amplitude indicating mitigation of blast effects.
(5) The pressure in the skin (adjacent to the foam) is lower when the foam pads are used (prior to occurrence of the gap between foam and skin).
(6) The pressure is amplified as it enters from skin to bone due to higher acoustic impedance.

These observations were based on the simulation of the model not containing any retention system. If the strap is modeled, the restrained interaction between the helmet and the head is expected to alter the results.

Another important aspect is the model for the foam. The fabric cover is expected to have a significant effect on the deformation in the foam, and subsequent load transfer to the head. Modeling the foam into a soft and a hard layer instead of one single layer with average properties may also alter the wave propagation (magnitude and shape) as well.

REFERENCES

[1] Tham C., Tan V., Lee H., 2008, “Ballistic Impact of a KEVLAR Helmet: Experimental and Simulations”, International Journal of Impact Engineering, 35, pp. 304-318.

[2] Moss W., and King M., 2011, “Impact Response of US Army and National Football League Helmet Pad Systems”, LLNL-SR-464951, Lawrence Livermore National Laboratory.

[3] Grujicic M., Bell W., Pandurangan B., He T., 2010, “Blast-wave Impact-mitigation Capability of Polyurea when Used as Helmet Suspension-pad Material”, Materials and Design, 31, pp. 4050-4065.

[4] Chavko M., Watanabe T., etc, 2011, "Relationship between Orientation to a Blast and Pressure Wave Propagation inside the Rat Brain", Journal of Neuroscience Method, 195, pp. 61-66.

[5] Grujicic M., Bell W., Pandurangan B, and Glomski P., 2011, "Fluid/Structure Interaction Computational Investigation of Blast-Wave Mitigation Efficacy of the Advanced Combat Helmet", Journal of Materials Engineering and Performance, 20(6), pp. 877-893.

[6] Slavik T., 2009, "A coupling of Empirical Explosive Blast Loads to ALE Air Domains in LS-DYNA", 7th European LS-DYNA Conference.

[7] Ganpule S., Gu L., Alai A. and Chandra N, 2012, "Role of helmet in the mechanics of shock wave propagation under blast loading conditions", Computer Methods Biomechanics and Biomedical Engineering, 15 (11) pp. 1233-1244.

[8] Zheng J., March, 2012, "Helmet Testing Related Research and Development", Presentation at NRC meeting, Washington DC.

[9] Annaidh A., Bruyere K., Destrade, M, etc, 2012, "Characterization of the anisotropic mechanical properties of excised human skin", Journal of the Mechanical Behavior of Biomedical Materials, 5, pp 138-148.

[10] Kleiven S, 2006, **"**Evaluation of head injury criteria using a finite element model validated against experiments on localized brain motion, intracerebral acceleration, and intracranial pressure**",** UCrash, 11 (1), pp 65-79.

[11] Panzer M., Myers B., Capehart B, and Bass C., 2012, "Development of a Finite Element Model for Blast Brain Injury and the Effects of CSF Cavitation", Annals of Biomedical Engineering, 40 (7), pp. 1530-1544.

[12] Herbert E., Balibar S., and Caupin F, 2006, "Cavitation pressure in water", Physical Review E, 74.

[13] Caupin F, and Herbert E, 2006, "Cavitation in water: a review", Comptes Rendus Physique, 7, pp. 1000-1017.

[14] Ganpule S., Alai A., Plougonven E., and Chandra N., 2012, "Mechanics of blast loading on the head models in the study of traumatic brain injury using experimental and computation approaches", Biomech Model Mechanobiol.

[15] Bowen I., Fletcher E. and Richmond D., 1968, "Estimate of Man's Tolerance to the Direct Effects of Air Blast", DASA-2113, Defense Atomic Support Agency, Washington, D.C.

[16] Schwer L, 2010, "A Brief Introduction to Coupling Load Blast Enhanced with Multi-Material ALE: The Best of Both Worlds for Air Blast Simulation', LS-DYNA Forum, Bamberg.

1 DEFENSE TECHNICAL
(PDF) INFORMATION CTR
DTIC OCA

2 DIRECTOR
(PDF) US ARMY RESEARCH LAB
RDRL CIO LL
IMAL HRA MAIL & RECORDS MGMT

1 GOVT PRINTG OFC
(PDF) A MALHOTRA

1 NATICK SOLDIER RSRCH DEV AND
(PDF) ENGRNG CTR
M G CARBONI

4 NATICK SOLDIER RSRCH DEV AND
(PDF) ENGRNG CTR
M CODEGA
R DILALLA
J WARD
P CUNNIFF

1 PROG EXECUTIVE OFC SOLDIER
(PDF) J ZHENG

4 SOUTHWEST RSRCH INST
(PDF) T HOLMQUIST
G JOHNSON
C ANDERSON JR
S CHOCRON

1 INST FOR DEFNS ANLYS
(PDF) Y MACHERET

35 DIR USARL
(PDF) RDRL SLB W
P GILLICH
J GURGANUS
W MERMAGEN
K RAFAELS
RDRL WMM A
D O'BRIEN
T PLAISTED
E WETZEL
RDRL WMM B
T BOGETTI
B CHEESEMAN
B LOVE
P MOY
C YEN
RDRL WMM D
L VARGAS
S WALSH
RDRL WMP
S SCHOENFELD
RDRL WMP B
A DAGRO
A GUNNARSSON
C HOPPEL
P MCKEE
S SATAPATHY
T WEERASOORIYA
T ZHANG
K ZIEGLER
RDRL WMP C
R BECKER
T BJERKE
M J GRAHAM
C MEREDITH
RDRL WMP D
R DONEY
C RANDOW
B SCOTT
RDRL WMP E
S BARTUS
M BURKINS
P SWOBODA
RDRL WMP F
N GNIAZDOWSKI
R GUPTA
RDRL WMS
M VANLANDINGHAM